Journal of Molecular Graphics and Modelling 27 (2008) 401–407

Contents lists available at ScienceDirect

Journal of Molecular Graphics and Modelling

journal homepage: www.elsevier.com/locate/JMGM

Structure and dimerization of the teleost transmembrane immunoglobulin region

Antonello Merlino [a,*], Sonia Varriale [a,b], Maria Rosaria Coscia [b], Lelio Mazzarella [a,c], Umberto Oreste [b]

[a] Department of Chemistry, University of Naples 'Federico II', Via Cinthia, I-80126, Naples, Italy
[b] Institute of Protein Biochemistry, CNR, Via Pietro Castellino 111, I-80131, Naples, Italy
[c] Institute of Biostructures and Bioimages, CNR, Via Mezzocannone 16, I-80134, Naples, Italy

ARTICLE INFO

Article history:
Received 15 May 2008
Received in revised form 8 July 2008
Accepted 10 July 2008
Available online 22 July 2008

Keywords:
Membrane protein
Transmembrane domain
Molecular dynamics
Explicit lipid bilayer
Protein–protein interactions
Helix–helix packing

ABSTRACT

The immune system cells express activating receptors, which consist of a dimeric ligand-binding molecule associated with a signal transducing dimer. The communication between the receptor partners depends primarily on the interactions between their membrane-embedded segments. In the B cell receptor (BCR) the sequence traversing the lipid bilayer of the immunoglobulin (IgTM) is highly conserved among species. We have investigated the association of the IgTM regions of the BCR of the Antarctic teleost *Chionodraco hamatus*. The nucleotide sequence of the entire immunoglobulin chain has been determined and the length, polarity, and structure of the IgTM region have been thoroughly analyzed. Structural models of the IgTM homodimer were also obtained by performing several MD simulations in a lipid bilayer using, as a starting model, two copies of the IgTM helix placed at various relative orientations and distances. Despite a certain degree of conformational heterogeneity, the predicted models of the IgTM homodimer display similar packing interfaces, characterized by a high degree of surface complementarity. The residues presumably responsible for the interaction and, consequently for the receptor stability have been identified in this manner.

1. Introduction

Membrane proteins play an essential role in several cellular functions, including cell division, intra- and inter-cellular signaling, macromolecule and energy transport. Although membrane proteins can be exceedingly complex, their transmembrane (TM) regions are often relatively simple. Two different basic architectures can be attributed to the TM regions: the α-helix-bundle and the β-barrel [1]. Biogenesis of helix-bundle and β-barrel proteins follows different steps. In particular, ribosomes making helix-bundle proteins bind, during translation, to a protein complex known as translocon that assures the translocation of the nascent chain in the endoplasmic reticulum where it folds [2]. The protein then moves to the lipid bilayer as monomer or dimer depending on its hydrophobicity and tendency to aggregate.

The function of membrane proteins often depends on the interactions between their transmembrane regions [3]. The types of helix–helix interactions determining the structure of the TM region are sequence specific. The helix–helix assembly can be driven by van der Waals contacts [4,5], but electrostatic interactions [6] as well as hydrogen bonds [7] are sometimes observed. Specific TM helices packing motifs have been identified: the GxxxG and AxxxA motifs, present in the middle region of associated TM helices [8,9] and the SxxSSxxT or SxxxSSxxT motifs [10]. Examples of membrane proteins whose structure and assembly depend on helix–helix packing in the lipid bilayer include the homodimeric Rhodopsin [11,12], the glycophorin A (GpA) [13], the cell death factor BNIP3 [14].

Due to the difficulty in crystallizing membrane proteins for X-ray diffraction studies, multidisciplinary approaches that combine experimental and computational techniques are frequently used to gain insights into the structures of TM domains and to analyze the energetically favorable and tightly packed transmembrane α-helices [15]. Computational methods have been used to identify the interactions between TM helices when biochemical and biophysical data are not available. In this respect, molecular dynamics simulations have been demonstrated to be a very useful approach to provide a better understanding of TM helices association [16,17]. Dodecane has most often been used for the simulations to create a hydrophobic environment [18]. Recently, a more appropriate environment for many membrane proteins has been produced by using lipid molecules organized in a pre-

* Corresponding author. Tel.: +39 081674276; fax: +39 081674090.
E-mail address: antonello.merlino@unina.it (A. Merlino).

1093-3263/$ – see front matter © 2008 Elsevier Inc. All rights reserved.
doi:10.1016/j.jmgm.2008.07.001

equilibrated bilayer system: dodecyl phophocholine (DPC), dimyristoyl phophatidylcholine (DMPC), palmitoyl oleoyl phosphatidylcholine (POPC), dipalmitoyl phosphatidylcholine (DPPC), palmitoyl linoleyl phosphatidylcholine (PLPC) [16,17].

Also membrane protein complexes such as immune receptors have been recently investigated [19–21]. They share a distinctive assembly consisting of a ligand-binding molecule non-covalently associated with a signal transducing dimer, that carries cytoplasmic phosphorylation motifs [19]. In particular, within the T cell receptor αβ heterodimer, the ζζ dimer interactions have been well characterized [20]. At present, there are no data available about the B cell antigen receptor complex (BCR), the molecule responsible for the first step of immune response cascade. BCR is composed of a membrane-bound immunoglobulin molecule (Ig), consisting of two covalently linked heavy chains (IgH) and two light chains (IgL), associated with the transducing molecular partner formed by the disulphide bridged heterodimer Igα/Igβ [22]. The two covalently linked heavy chains wherein the extracellular environment traverse the lipid bilayer and three amino acid residues lean out of the cell membrane in the cytoplasm. The region of Ig embedded in the lipid bilayer (IgTM) is highly conserved among species and contains a sequential motif common to all immune receptors, known as the CART (conserved antigen receptor transmembrane) motif [23]. Although it is well known that the IgTM domain is crucial either for the BCR assembly or for the signal transduction, little is known about the structure of this region.

We have investigated the association of the IgTM regions in the BCR of *Chionodraco hamatus*, a fish living in the Antarctic sea, which represents the model species we have chosen for studying immunity. The primary sequence of the Ig was obtained. Using different computational methods, the length and the polarity of the α-helical IgTM region within the cell membrane were predicted, and a molecular model was built. The stability of the model was evaluated by molecular dynamics (MD) simulations performed both in water and in lipid bilayers. Models for the association of two IgTM helices were also investigated. Moreover, the results of the MD simulations were discussed on the bases of experimental data collected on the IgTM region of mammals.

2. Experimental methods

2.1. Cloning and sequencing of the C. hamatus IgH chain

Total RNA was isolated from the head kidney of a *C. hamatus* specimen, and subjected to reverse transcription using an oligo (dT) primer linked to an appropriate adapter (oligodT-AP: 5′-CGGAGATCTCCAATGTGATGGGAAATTCTTTTTTTTTTTTTTTT-3′). Double-stranded cDNA was amplified using a 5′ primer (5′-CTATAGGACAGGACTGC-3′) complementary to a sequence in the leader region of a related species (*Trematomus bernacchii*) and a 3′ primer (5′-CGGAGATCTCCAATGTGATGGGAAATTC-3′) complementary to the adapter. The amplification was performed as follows: 94 °C for 2 min, 30 cycles of 94 °C (1 min), 61 °C (1 min), and 72 °C (1 min) with a final extension at 72 °C for 10 min. The PCR products were then analyzed on 1% agarose gel: two bands were observed, one corresponding to the secreted form (1500 bp) and a second one, of the expected size of 1000 bp, corresponding to the membrane-bound form. Both were cloned into pCRII-TOPO vector (Invitrogen). Sequences of positive clones were determined with an ABI PRISM 3100 automated sequencer at PRIMM (Naples, Italy).

The accession number for the sequence encoding the secreted form is EU192078 and that for the sequence encoding the membrane form is EU192079.

2.2. Homology modeling

Sequence similarity searches were performed using the data from Swiss-Prot [24] and Protein Identification Resource (PIR) databanks [25]. The transmembrane region was predicted using TMpred (http://www.ch.embnet.org/software/TMPRED_form.html) [26] and HMMTM (http://biophysics.biol.uoa.gr/HMM-TM/index.jsp) [27] tools. Secondary structure predictions of the TM region were performed using the GOR program [28]. Models of *C. hamatus* IgTM region were built with the program 3D-PSSM (http://www.bmm.icnet.uk/∼3dpssm) [29], using the structure of the helix H of the photosynthetic reaction center of *Rhodobacter sphaeroides* as a template (sequence identity 33%). The structure was validated with PROCHECK [30], and a summary table of the output is reported in Table 1.

MD simulations in water and in the POPC bilayer have been performed to evaluate the stability of the model. POPC is a good mimic of the in vivo environment. It was chosen because it includes both a saturated (C16) and an unsaturated (C18) fatty acid, thus better resembling the cell membrane composition and thickness. The simulations in water have been performed simply to compare the different approaches.

Furthermore, in order to study the spontaneous formation of a parallel IgTM homodimer, four different initial configurations, in which the relative positions of the two helices were slightly varied, were built using the program O [31] and submitted to MD simulations both in water and in POPC environments. The first dimer was generated with the helix axes perfectly aligned. This initial construction was used to generate three other configurations by rotating one helix around its own axis of a few degrees, and by translating the same helix of a few Å. In all cases the distances between the centers of mass of the two helices were in the range 14–16 Å. The minimum distance between atoms belonging to the two helices was 5.2 Å.

2.3. Molecular dynamics simulations

All the computer simulations reported in this study were performed using GROMACS 3.2 package [32] and the GROMOS96 force field. The starting models were immersed in different boxes containing 3500–16,000 simple-point-charge water molecules. The ionization state was set to mimic a neutral pH environment. The overall charge of the system was neutralized by adding the appropriate number of ions 7 Å farther from the protein surface. In the first step of the equilibration process, the solvent was relaxed by energy minimization followed by a 20 ps MD at 300 K. The overall system was then minimized without restraints, before the productive run. All bond lengths were constrained by Lincs [33]. Newton's equations of motion were integrated with a time step of 2 fs and atomic coordinates were saved for analyses every 0.5 ps. A dielectric constant of 1 was used. A cut-off of 14 Å was used for the

Table 1
Procheck summary

Ramachandran plot	
Residues in core region	100.0%
Residues in generously allowed regions	0.0%
Residues in disallowed regions	0.0%
Bad contacts	0
G-factors	
Dihedrals	0.18
Covalent	0.16
Overall	0.19
M/c bond lengths within limits	99.3%
M/c bond angles within limits	94.9%

treatment of both electrostatic and Lennard–Jones interactions. All systems were simulated in the isobaric–isothermal (NPT) ensemble at 300 K, using periodic boundary conditions in the three coordinate directions. The pressure was controlled using the Berendsen algorithm at 1 bar with a coupling constant $\tau_p = 1$ ps at 300 K. The temperature was kept constant using the Berendsen thermostat with a coupling constant $\tau_p = 1$ ps [34].

The process of model insertion in the lipid bilayer and the MD runs in lipid environments were performed as suggested by other authors [35,36]. Specifically, the starting models were placed in a box containing a mixture of POPC lipids and water molecules. Before model insertion, the box contained 128 lipids and 3755 water molecules. After the protein insertion in the centre of the box, water molecules with oxygen atoms closer to 0.40 nm from a non-hydrogen atom of the protein, and lipid molecules with at least one atom closer to 0.4 nm from a non-hydrogen atom of the model were removed. Removal of these atoms introduces small voids between the model and water or lipid molecules that are easily removed during the first steps of the equilibration process. During this step, a few simulations of 10 ps were performed, with the atomic coordinates of the protein restrained to the initial positions. This resulted in final systems containing 110 lipids and about 3730 water molecules. For the simulations in POPC, the Part Mesh Ewald (PME) method [37] was used for the treatment of electrostatic interactions for atoms at a distance greater than 9 Å. The force field and the coordinates for POPC were downloaded from the Tieleman group web-site (http://mouse.bio.ucalgary.ca).

All the trajectories were estimated to assess the quality of the simulations using GROMACS routines and in-house programs. We evaluated the surface complementarity by calculating the statistics S_c value [38], and by quantifying the geometrical packing of protein interfaces on representative models using the CCP4 suite [39]. The global structural stability of the simulations was confirmed by analyzing several structural parameters (i.e. secondary structure, radius of gyration and total number of hydrogen bond) as a function of time. The stability of the simulations was also assessed by measuring the convergence in the essential space. Essential degrees of freedom were extracted from the trajectories according to the essential dynamics method [40]. The convergence in the essential space (first 10 eigenvectors) was checked by calculating the root mean squared inner products (RMSIP) between two halves of the trajectory (the RMSIP values are >0.59) as previously reported [41,42] and by measuring mean squared fluctuation versus time block analysis. The RMSIP is defined as:

$$\sqrt{\frac{1}{10}\sum_{i=1}^{10}\sum_{j=1}^{10}(\eta_i^a\eta_j^a)^2}$$

where η_i^a and η_j^a are the ith and jth eigenvectors, obtained from diagonalization of the covariance matrix, from the first and second half of the trajectory, respectively (for further details see references [41,42]).

3. Results

3.1. Analysis of the membrane-bound domain

The transcripts of both the secreted and membrane-bound IgM heavy chain were cloned and sequenced. By sequence analysis the membrane form was shown to posses a different carboxyl-terminal region, which is responsible for the interaction with the cell membrane. This region showed the longest size (79-amino acid residues) among all species (ranging between 43 residues in mammals and 49 residues in puffer fish). Based on comparison with other vertebrates, the identity percentage for the overlapping regions, ranged between 87.5 (spotted wolfish) and 53.3 % (man).

The prediction of the extra cellular, membrane-crossing and cytoplasmic regions obtained by both tools mentioned in the methods, were similar, and are reported in Fig. 1, where the *C. hamatus* membrane-bound region is aligned together with those from other vertebrates available in data banks. The membrane-crossing region as well as the cytoplasmic tail are highly conserved, whereas the extracellular spacer is highly divergent either between teleosts and mammals or within teleosts. The membrane-crossing region, predicted to have an α-helical conformation, includes the majority of the conserved positions (in bold in Fig. 1).

3.2. Homology modeling and molecular dynamics of a single IgTM helix

A molecular model of the *C. hamatus* IgTM region, corresponding to the sequence NMGSTAITFILLFLITLLFSIGTTAFKVK, was built using the helix H of the photosynthetic reaction centre of *R. sphaeroides* as a template (sequence identity 33%). The modeled IgTM structure consists of an extended, nearly ideal, α-helix. As shown in Fig. 2, the conserved residues (Thr5, Phe9, Leu12, Thr16, Phe19 and Thr24, according to the numbering scheme used in this paper) are all located on one face of the helix and are solvent exposed.

As a preliminary investigation of the IgTM helix–helix association, the stability of the IgTM structure in POPC was monitored by performing a 50-ns-duration simulation. The IgTM molecule remained folded and close to the ideality during the simulation timescale, as suggested by the analysis of secondary structure, radius of gyration, helix radius and total number of hydrogen bonds as a function of time. The C_α root mean square

```
                                                      Extracellular       /      membrane      /cyt
                   1        10        20        30        40        50        60        70
C.hamatus          DKLGVLCPCHTCDDKVGAHRPCHIHDDSNQTDIDKKVEGYDMGYTEVEEDNMGSTAITFILLFLITLLFSIGTTAFKVK
Spotted wolffish                                    VYQQVCQCNSAME-EEDNMGNTALTFILLFLFTLLFTIGTTAFKVK
Torafugu                                        DFLIETN----SSAVHAEEDNMGDTAITFIFLFLITLLFSIATTAFKIK
Pufferfish                                      EFLIETNYHWSCSTVDTEEDNMGDTAITFIFLFLLTLLFSIGTTAFKIK
Zebrafih                                        AWIVWIE-HPLFEPINADDSGIANTAVTFIFLFLITLFYSIGATFVKVK
Carp                                            AVIVWLE-HPLYEASDTDDSGIANTAITFVFLFLITLFYSIGATFVKVK
Atlantic salmon                                  CLVLTD-CPCSNTIETDRDSMGKTAFTFIILFLITLLYGVGATAIKVK
Rainbow trout                                   DCLVLTD-CPCSNTMETDRDSMGKTAFTFIILFLITLLYGVGATAIKVK
Channel catfish                                  CI-WST-EIFHYEMEMDDDNMANTALTFVFLFLITLFYSIGVTVFKVK
Atlantic cod                                    AFLVLTE-SQWSNAVDGQQDSMQSTLNTFIILFLITLVYSIGTTAIKIR
Mouse                                                 EGE--VNAEEEGFENLWTTASTFIVLFLLSLFYSTTVTLFKVK
Man                                                   EGE--VSADEEGFENLWATASTFIVLFLLSLFYSTTVTLFKVK
```

Fig. 1. Sequence alignment of IgTM region of different species. Conserved residues are shown in bold.

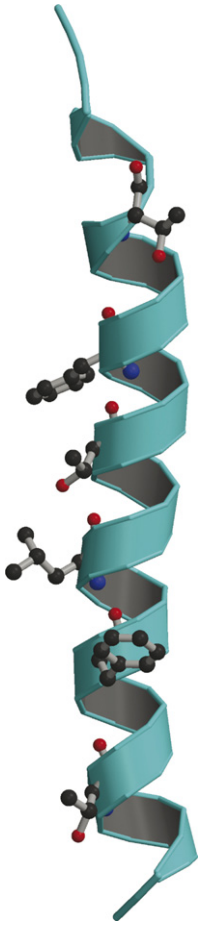

Fig. 2. Ribbon diagram of IgTM α-helix. Conserved residues are shown in ball-and-stick.

deviation (RMSD) of the structure *versus* the starting model is constant at about 2 Å. The hydrophobic patch (residue 9–19) of the α-helix is completely immersed in the membrane and the charged terminal portions (residues 1–4 and 27–29) are anchored to the water-membrane polar interface.

In order to characterize the structure of the IgTM helix in the different environments, two simulations in water were also performed. The results of these simulations revealed that a local unfolding of the N- and C-termini of the α-helix occurred in water.

3.3. IgTM helix–helix association, structure and stability

In order to study the spontaneous formation of a parallel IgTM homodimer, four configurations, which differ for the relative positions of the two helices, were generated and used in MD studies performed in water and in POPC.

Eight simulations were performed in POPC bilayer (from 15 to 50 ns per simulation, for a total of more than 150 ns), and all showed the formation of a stable homodimer. This result is not surprising since spontaneous helix–helix aggregations were already observed in nanosecond time simulations, providing that the starting configurations are not too far away [13,14]. On the other hand, 4 out of 10 simulations performed in water, for a total of about 120 ns, did not produce a parallel pairing of the two helices. In such cases, the resulting structures were characterized by an antiparallel packing of the two helices (two cases), separated folded α-helices (one case) or helices interacting in an irregular fashion (one case).

Fig. 3 depicts views of six representative models obtained by the POPC simulations (panels A and B) and of the six models obtained by MD simulations in water (panels C and D). In the figure, one helix is fixed in the same position for each structure so that the differences in the orientation between the helices can be easily grasped. The root mean square deviations of the residues involved in the interfacial region (residues 12–19 of the two chains) among the different models obtained from the POPC simulations fall in the range from 0.4 to 3.3 Å. These data indicate that the interfaces which stabilize the homodimers obtained by the simulations in POPC are similar to each other (Fig. 3A and B). This similarity suggests that the models obtained can be a plausible representation for the IgTM assembly in the BCR.

On the contrary, the homodimers obtained in water presented a larger structural variability (Fig. 3C and D). The helices interacted through different faces. In some cases, a deep distortion of the helical structure occurred. The root mean square deviation of residues 12–19 of the two chains among these structures covered the range from 2.1 to 5.0 Å.

The MD simulations in the lipid environment were investigated to single out the relevant interactions that lead to IgTM homodimer association and structural stability. As expected, the pairing of the two helices is driven by hydrophobic interactions. In fact, the total solvent accessible surface area of the hydrophobic residues rapidly changes its value from an average of 1100 $Å^2$ to an average of about 950 $Å^2$, whereas the solvent exposed area of hydrophilic residues remains practically unchanged at about 900 $Å^2$. The time evolution of the secondary structure elements, the gyration radius of the C_α atoms and the number of hydrogen bonds of each separated helix indicate that the monomers retain their structure during the helix–helix association, except for the expected unwinding at the terminal tails. The rise per residue of the helices ranges from 1.32 to 1.61 and in most cases is close to the ideal value of 1.5.

The total accessible surface area, the number of hydrogen bonds (37–40) and the surface complementarity sc (0.63–0.69) of the homodimeric IgTM models show that they have a compact structure. The two helices are formed by an average of 22 residues, two residues more than those required to span the 30 Å of the hydrophobic membrane. The presence of longer stretches of residues in some cases is associated to a little helix distortion (helix kink). The helix kink results in an increased radius of gyration and in a decreased number of hydrogen bonds per helix. Interfacial residues involved in the helix–helix recognition have been identified by visual inspection of the MD trajectories and by the plot of the distance between side chain atoms of residues belonging to the two chains as function of time. The intermolecular interface comprises 6–8 residues. The interfacial region lacks intermolecular hydrogen bonds. The two helices interact essentially *via* van der Waals interactions (Fig. 4A–C) between the same interfacial residues Phe9, Leu12, Phe13, Leu14, Leu17 and Phe19 of the two chains. Although the mean intermolecular distances between these key residues change across the simulations, specific contacts that drive the IgTM recognition can be identified. The most conserved intermolecular interaction forms between side chains of residues Phe13 and Leu12 (Fig. 4A and B). Furthermore, a π–π interaction between the two Phe19 is intermittently observed, since the two aromatic rings are parallel at a distance of 4.3 Å [43]. Other interactions, often observed, involve the side chains of residues Leu12, Phe13, and Leu14 with Phe9 (Fig. 4C). Finally, residues Phe9–Phe9, Leu17–Phe19 and Phe13–Leu14 can be in close contact.

In the final homodimeric models, the N- and C-termini are solvent exposed. At the C-terminal tails, Lys27 and Lys29 of the two chains make favorable interactions with oxygen atoms of the POPC

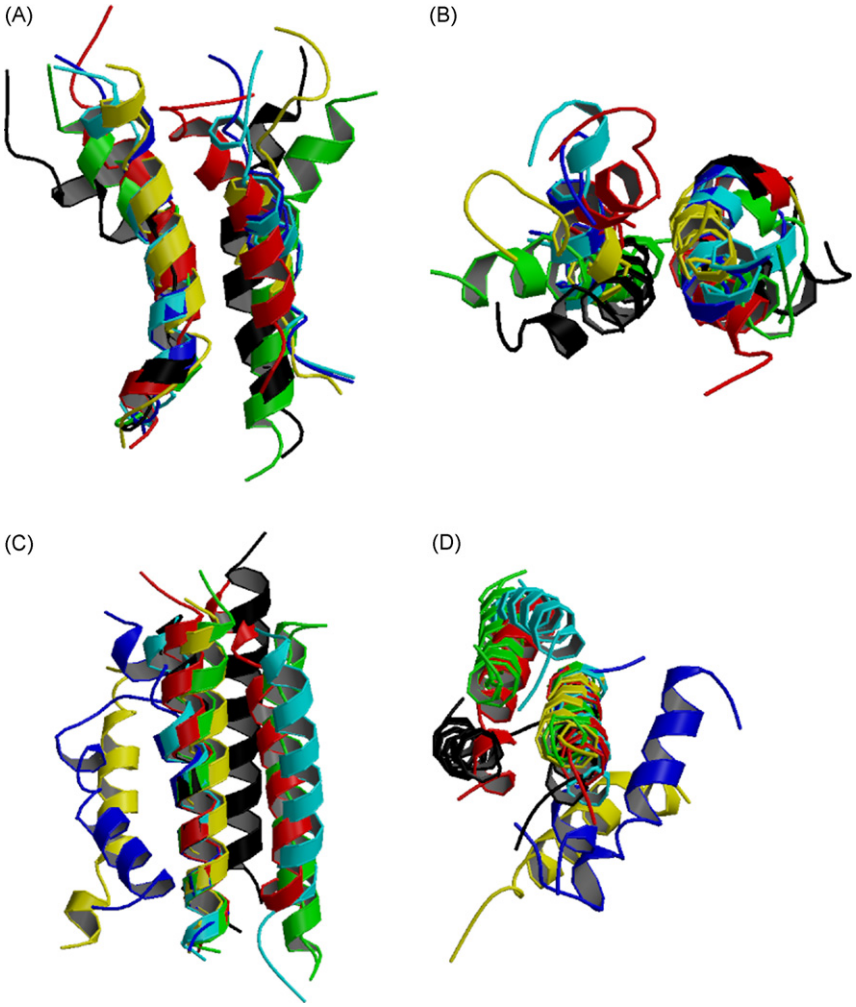

Fig. 3. Structural comparison between the IgTM homodimers obtained from simulations in different environments. Six representative structures obtained from POPC simulations are shown in panel A and B, whereas six structures obtained from water simulations are shown in panel C and D.

molecules on the surface of the lipid bilayer, thus anchoring the dimer to the membrane. In fact we noted that during the simulations, these residues were allowed to move but constantly facing the lipid headgroups. At the amino-terminus an Asn residue seems to interact with the external phosphate groups.

4. Discussion

The difficulty of obtaining experimental structures of membrane protein molecules has stimulated the application of theoretical procedures as a tool to provide basic clues regarding the proteins assembly in membrane. In particular, MD simulations can provide useful insights into the factors governing helix–helix association in lipid bilayers. Although incomplete sampling, inaccurate force fields, and approximate treatment of long-range interactions intrinsically limit these studies, intriguing results on the mechanisms of TM helix recognition have been recently reported [13,14,44–47].

In this paper, we used a computational approach that combines homology modeling and molecular dynamics simulations to predict the structure of the transmembrane region of the immunoglobulin and analyzed the interactions stabilizing its association in the membrane. The results are relevant to the problem of receptor stability, signal transduction cascade inside the cell, and could also be used to design therapeutic agents for potential pharmaceutical applications. We have focused on the transmembrane region of *C. hamatus* Immunoglobulin, whose sequence is reported here for the first time. The results indicate that the immunoglobulin transmembrane region adopts an α-helical structure, which is significantly more stable in the lipid bilayer than in solution. The MD simulations also suggest that individual IgTM helices are stable, as observed in the case of glycophorin A [18].

Moreover, several simulations independently carried out on the IgTM homodimers reveal that the spontaneous formation of the transmembrane Ig helix–helix dimer of IgTM is more likely to form inside the lipid bilayer, rather than in water, where a number of antiparallel/non-physiological structures have been also obtained. These data suggest that in the case of BCR, the lipid environment does exert a major effect on the TM helix packing.

Given the high sequence similarity between the IgTM region of *C. hamatus* and that of other species, our results could be extended to the folding and assembly of different species BCR. The present data suggest that the parallel helix–helix structure of IgTM in BCR is stabilized basically by the van der Waals interactions of the two Phe19 side chains and by the insertion of Leu12 side chain of one chain between Phe9 and Phe13 of the partner chain at the helix–helix interface. The tight packing of these side chains results in a small (about 150 $Å^2$), but highly complementary (sc = 0.65) contact surface area, that lacks inter-helical hydrogen bonds. These data

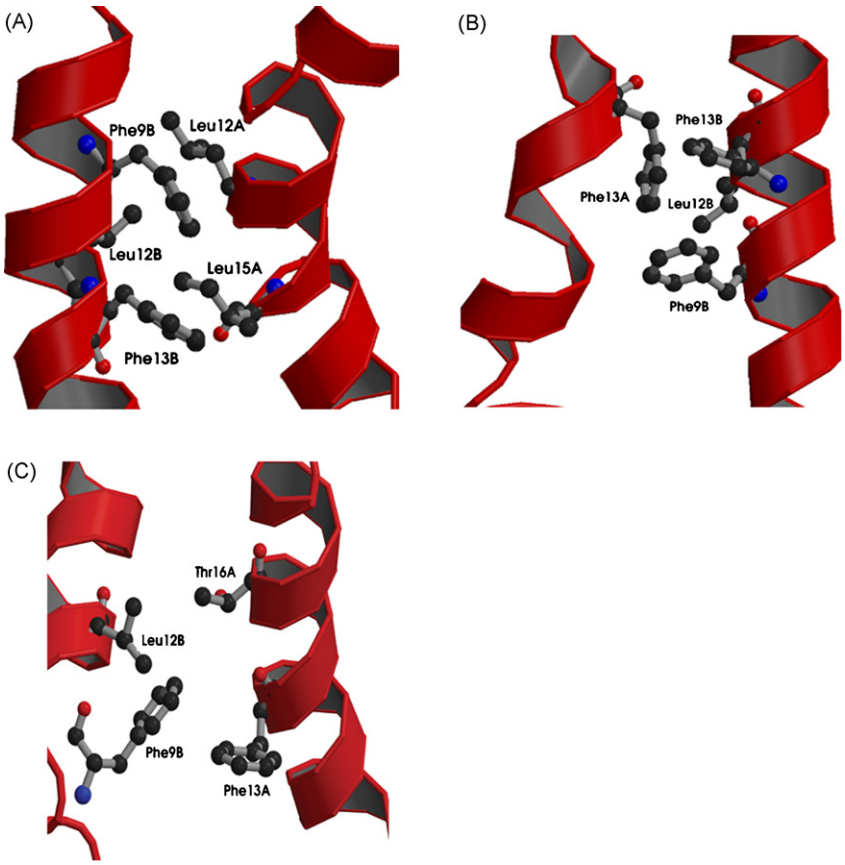

Fig. 4. Residues determining the structure and stability of the IgTM homodimers in representative models obtained from POPC simulations.

are in agreement with mutagenesis studies that revealed that the substitution of polar residues at the N-terminus (residues 4–8 in our numbering scheme) of human IgM with alanine or valine does not affect the BCR association and signaling [48–50], whereas the double mutation of residues 19 and 20 (Tyr-Ser in mouse, Phe-Ser in *C. hamatus*) to Val, in the transmembrane domain of mouse membrane Ig, weakens the association of Ig with Igα/Igβ and destabilizes the BCR structure [51]. It should be recalled that both the single mutations Y19F and S20A of mouse IgM do not hamper the signal transduction [49,52]. These observations strongly validate the final model obtained for the dimer, which highlights the inter-helix direct interactions between the aromatic side chains of residue 19 as a stabilizing motif for the dimer. Interestingly, these data are also in line with a recent suggestion that the aromatic nature of Trp, Tyr and Phe can be a critical feature in self-association of TM helices [20,53]. Vice versa, the simulations also suggest that the three conserved threonines (residues 5, 16 and 24 in our numbering scheme) provide little assistance in the association of the helices. This result agrees with mutagenesis data which show that the replacement of Thr5 or Thr16 with a hydrophobic residue is well tolerated [52,54], and that the point mutation of T24V does not alter the BCR association, although it decreases the sensitivity of signal transduction [52,55]. This also agrees with the finding that, although serine and threonine are found in TM helices more frequently than other polar residues, they prefer to form intra helical hydrogen bonds to main-chain carboxyl oxygen rather than inter-helical contacts [55,56]. Altogether these results strengthen the hypothesis that the MD homodimeric structure may indeed depict the IgTM association.

Interestingly, in some models one of the helices immersed in the bilayer is kinked in the middle. It should be noted that this result has been obtained without imposing helix kinks. This finding could be explained by the 'hydrophobic match' effect [57] that may affect the protein conformation, inducing a conformational change in the helices. In the case of the IgTM, an important role in driving the helix kink could be also played by the interactions that the lysine residues at the C-terminal regions form with the oxygen atoms of the lipid bilayer. Notably, C-terminal residues have also been considered important for BCR structure/function by other authors. In fact, experimental data have shown that the deletion of the KVK region (residues 27–29 of our model) produces a loss of mouse BCR function [52,58], and that the substitution of the lysines 27 and 29 with negatively charged residues affects the signal transduction, whereas the replacement of the lysines with positively charged residues does not [49,50].

Acknowledgment

The Italian National Program financially supports this study for Antarctic Research (PNRA), Project 2005.1.2.

References

[1] A. Elofsson, G. von Heijne, Membrane protein structure: prediction vs reality, Annu. Rev. Biochem. 76 (2007) 125–140.
[2] S.H. White, G. von Heijne, Transmembrane helices before, during, and after insertion, Curr. Opin. Struct. Biol. 15 (2005) 378–386.
[3] B.J. Bormann, D.M. Engelman, Intramembrane helix-helix association in oligomerization and transmembrane signalling, Annu. Rev. Biophys. Biomol. Struct. 21 (1992) 223–242.
[4] K.R. MacKenzie, J.H. Prestegard, D.M. Engelman, A transmembrane helix dimer: structure and implications, Science 276 (1997) 131–133.
[5] M.A. Lemmon, J.M. Flanagan, J.F. Hunt, B.D. Adair, B.J. Bormann, C.E. Dempsey, D.M. Engelman, Glycophorin A dimerization is driven by specific interactions between transmembrane alpha-helices, J. Biol. Chem. 267 (1992) 7683–7689.

[6] H. Gratkowski, J.D. Lear, W.F. DeGrado, Polar side chains drive the association of model transmembrane peptides, Proc. Natl. Acad. Sci. USA 98 (2001) 880–885.
[7] F.X. Zhou, M.J. Cocco, W.P. Russ, A.T. Brunger, D.M. Engelman, Interhelical hydrogen bonding drives strong interactions in membrane proteins, Nat. Struct. Biol. 7 (2000) 154–160.
[8] G. Kleiger, R. Grothe, P. Mallick, D. Eisenberg, GXXXG and AXXXA: common alpha-helical interaction motifs in proteins, particularly in extremophiles, Biochemistry 41 (2002) 5990–5997.
[9] D. Schneider, D.M. Engelman, Motifs of two small residues can assist but are not sufficient to mediate transmembrane helix interactions, J. Mol. Biol. 343 (2004) 799–804.
[10] J.P. Dawson, J.S. Weinger, D.M. Engelman, Motifs of serine and threonine can drive association of transmembrane helices, J. Mol. Biol. 316 (2002) 799–805.
[11] T. Okada, I. Le Trong, B.A. Fox, C.A. Behnke, R.E. Stenkamp, K. Palczewski, X-Ray diffraction analysis of three-dimensional crystals of bovine rhodopsin obtained from mixed micelles, J. Struct. Biol. 130 (2000) 73–80.
[12] A.B. Patel, E. Crocker, P.J. Reeves, E.V. Getmanova, M. Eilers, H.G. Khorana, S.O. Smith, Changes in interhelical hydrogen bonding upon rhodopsin activation, J. Mol. Biol. 347 (2005) 803–812.
[13] M. Mottamal, J. Zhang, T. Lazaridis, Energetics of the native and non-native states of the glycophorin transmembrane helix dimer, Proteins 62 (2006) 996–1009.
[14] Y.A. Vereshaga, P.E. Volynsky, J.E. Pustovalova, D.E. Nolde, A.S. Arseniev, R.G. Efremov, Specificity of helix packing in transmembrane dimer of the cell death factor BNIP3: a molecular modeling study, Proteins 69 (2007) 309–325.
[15] J.A. Leeds, D. Boyd, D.R. Huber, G.K. Sonoda, H.T. Luu, D.M. Engelman, J. Beckwith, Genetic selection for and molecular dynamic modeling of a protein transmembrane domain multimerization motif from a random Escherichia coli genomic library, J. Mol. Biol. 313 (2001) 181–195.
[16] J.M. Cuthbertson, P.J. Bond, M.S. Sansom, Transmembrane helix-helix interactions: comparative simulations of the glycophorin a dimer, Biochemistry 45 (2006) 14298–14310.
[17] T. Rog, K. Murzyn, M. Karttunen, M. Pasenkiewicz-Gierula, Nonpolar interactions between trans-membrane helical EGF peptide and phosphatidylcholines, sphingomyelins and cholesterol, Molecular dynamics simulation studies, J. Pept. Sci. 14 (2008) 374–382.
[18] J. Henin, A. Pohorille, C. Chipot, Insights into the recognition and association of transmembrane alpha-helices. The free energy of alpha-helix dimerization in glycophorin A, J. Am. Chem. Soc. 127 (2005) 8478–8484.
[19] M.E. Call, K.W. Wucherpfennig, Common themes in the assembly and architecture of activating immune receptors, Nat. Rev. Immunol. 7 (2007) 841–850.
[20] M.E. Call, J.R. Schnell, C. Xu, R.A. Lutz, J.J. Chou, K.W. Wucherpfennig, The structure of the ζζ transmembrane dimer reveals features essential for its assembly with the T cell receptor, Cell 127 (2006) 355–368.
[21] J. Feng, M.E. Call, K.W. Wucherpfennig, The assembly of diverse immune receptors is focused on a polar membrane-embedded interaction site, PLoS Biol. 4 (2006) e142.
[22] J. Hombach, T. Tsubata, L. Leclercq, H. Stappert, M. Reth, Molecular components of the B-cell antigen receptor complex of the IgM class, Nature 343 (1990) 760–762.
[23] K.S. Campbell, B.T. Backstrom, G. Tiefenthaler, E. Palmer, CART: a conserved antigen receptor transmembrane motif, Semin. Immunol. 6 (1994) 393–410.
[24] A. Bairoch, R. Apweiler, The SWISS-PROT protein sequence data bank and its supplement TREMBL, Nucleic Acids Res. 25 (1997) 31–36.
[25] K.E. Sidman, D.G. George, W.C. Barker, L.T. Hunt, The protein identification resource (PIR), Nucleic Acids Res. 16 (1988) 1869–1871.
[26] K. Hofmann, W. Stoffel, TMbase – a database of membrane spanning proteins segments, Biol. Chem. 374 (1993) 166.
[27] P.G. Bagos, T.D. Liakopoulos, S.J. Hamodrakas, Algorithms for incorporating prior topological information in HMMs: application to transmembrane proteins, BMC Bioinform. 7 (2006) 189.
[28] A. Kloczkowski, K.L. Ting, R.L. Jernigan, J. Garnier, Combining the GOR V algorithm with evolutionary information for protein secondary structure prediction from amino acid sequence, Proteins 49 (2002) 154–166.
[29] L.A. Kelley, R.M. MacCallum, M.J.E. Sternberg, Enhanced genome annotation using structural profiles in the program 3D-PSSM, J. Mol. Biol. 299 (2000) 499–520.
[30] R.A. Laskowski, M.W. MacArthur, M.D. Moss, J.M. Thorton, PROCHECK:, A program to check the stereochemical quality of protein structure, J. Appl. Crystallogr. 26 (1993) 283–291.
[31] T.A. Jones, M. Bergdoll, M. Kjeldgaard, O: a macromolecule modeling environment. In: C. Bugg, S. Ealick (Eds.), Crystallogr. Model Methods Mol. Des. [Pap Symp.]. Springer-Verlag Press, 1990, pp. 189–199.
[32] D. Van Der Spoel, E. Lindahl, B. Hess, G. Groenhof, A.E. Mark, H.J. Berendsen, GROMACS: fast, flexible, and free, J. Comput. Chem. 26 (2005) 1701–1718.
[33] H.J.C. Berendsen, J.P.M. Postma, W.F. van Gusteren, J. Hermans, Interaction Models for Water in Relation to Protein Hydration, Reidel, Dordrecht, 1981, pp. 331–342.
[34] H.J.C. Berendsen, J.P.M. Postma, W.F. van Gusteren, A. Di Nola, J.R. Haak, Molecular dynamics with coupling to an external heat bath, J. Chem. Phys. 81 (1984) 3684–3690.
[35] C. Kandt, W.L. Ash, D.P. Tieleman, Setting up and running molecular dynamics simulations of membrane proteins, Methods 41 (2007) 475–488.
[36] L. Vaccaro, K.J. Cross, J. Kleinjung, S.K. Straus, D.J. Thomas, S.A. Wharton, J.J. Skehel, F. Fraternali, Plasticity of influenza haemagglutinin fusion peptides and their interaction with lipid bilayers, Biophys. J. 88 (2005) 25–36.
[37] T. Darden, D. York, L. Pedersen, Particle mesh Ewald: An N·log(N) method for Ewald sums in large systems, J. Chem. Phys. 98 (1993) 10089–10092.
[38] M.C. Lawrence, P.M. Colman, Shape complementarity at protein/protein interfaces, J. Mol. Biol. 234 (1993) 946–950.
[39] Collaborative Computational Project, Number 4, The CCP4 suite: programs for protein crystallography, Acta Crystallogr. Sect. D 50 (1994) 760–763.
[40] A. Amadei, A.B.M. Linssen, H.J.C. Berendsen, Essential dynamics of proteins, Proteins 17 (1993) 412–425.
[41] A. Merlino, L. Vitagliano, M.A. Ceruso, L. Mazzarella, Subtle functional collective motions in pancreatic-like ribonucleases: from ribonuclease A to angiogenin, Proteins 53 (2003) 101–110.
[42] A. Merlino, L. Vitagliano, M.A. Ceruso, L. Mazzarella, Dynamic properties of the N-terminal swapped dimer of ribonuclease A, Biophys. J. 86 (2004) 2383–2391.
[43] S.K. Burley, G.A. Petsko, Amino-aromatic interactions in proteins, FEBS Lett. 203 (1986) 139–143.
[44] E. Sparr, W.L. Ash, P.V. Nazarov, D.T. Rijkers, M.A. Hemminga, D.P. Tieleman, J.A. Killian, Self-association of transmembrane alpha-helices in model membranes: importance of helix orientation and role of hydrophobic mismatch, J. Biol. Chem. 280 (2005) 39324–39331.
[45] J. Gumbart, Y. Wang, A. Aksimentiev, E. Tajkhorshid, K. Schulten, Molecular dynamics simulations of proteins in lipid bilayers, Curr. Opin. Struct. Biol. 15 (2005) 423–431.
[46] J. Henin, B. Maigret, M. Tarek, C. Escrieut, D. Fourmy, C. Chipot, Probing a model of a GPCR/ligand complex in an explicit membrane environment: the human cholecystokinin-1 receptor, Biophys. J. 90 (2006) 1232–1240.
[47] O. Samna Soumana, N. Garnier, M. Genest, Molecular dynamics simulation approach for the prediction of transmembrane helix-helix heterodimers assembly, Eur. Biophys. J. 36 (2007) 1071–1082.
[48] B.J. Cherayil, K. MacDonald, G.L. Waneck, S. Pillai, Surface transport and internalization of the membrane IgM H chain in the absence of the Mb-1 and B29 proteins, J. Immunol. 151 (1993) 11–19.
[49] A.C. Shaw, R.N. Mitchell, Y.K. Weaver, J. Campos-Torres, A.K. Abbas, P. Leder, Mutations of immunoglobulin transmembrane and cytoplasmic domains: effects on intracellular signaling and antigen presentation, Cell 63 (1990) 381–392.
[50] S.A. Grupp, K. Campbell, R.N. Mitchell, J.C. Cambier, A.K. Abbas, Signaling-defective mutants of the B lymphocyte antigen receptor fail to associate with Ig-alpha and Ig-beta/gamma, J. Biol. Chem. 268 (1993) 25776–25779.
[51] T.L. Stevens, J.H. Blum, S.P. Foy, L. Matsuuchi, A.L. DeFranco, A mutation of the mu transmembrane that disrupts endoplasmic reticulum retention. Effects on association with accessory proteins and signal transduction, J. Immunol. 152 (1994) 4397–4406.
[52] J.H. Blum, T.L. Stevens, A.L. DeFranco, Role of the μ immunoglobulin heavy chain transmembrane and cytoplasmic domains in B cell antigen receptor expression and signal transduction, J. Biol. Chem. 268 (1993) 27236–27245.
[53] N. Sal-Man, D. Gerber, I. Bloch, Y. Shai, Specificity in transmembrane helix-helix interactions mediated by aromatic residues, J. Biol. Chem. 282 (2007) 19753–19761.
[54] C.M. Pleiman, N.C. Chien, J.C. Cambier, Point mutations define a mIgM transmembrane region motif that determines intersubunit signal transduction in the antigen receptor, J. Immunol. 152 (1994) 2837–2844.
[55] J.A. Ballesteros, X. Deupi, M. Olivella, E.E. Haaksma, L. Pardo, Serine and threonine residues bend alpha-helices in the chi(1) = g(−) conformation, Biophys. J. 79 (2000) 2754–2760.
[56] T.M. Gray, B.M. Matthews, Intrahelical hydrogen bonding of serine, threonine and cysteine residues within alpha-helices and its relevance to membrane-bound proteins, J. Mol. Biol. 175 (1984) 75–81.
[57] T.M. Weiss, P.C. van der Wel, J.A. Killian, R.E. 2nd Koeppe, H.W. Huang, Hydrophobic mismatch between helices and lipid bilayers, Biophys. J. 84 (2003) 379–385.
[58] R.N. Mitchell, A.C. Shaw, Y.K. Weaver, P. Leder, A.K. Abbas, Cytoplasmic tail deletion converts membrane immunoglobulin to a phosphatidylinositol-linked form lacking signaling and efficient antigen internalization functions, J. Biol. Chem. 266 (1991) 8856–8860.